

Dual Mode Control of Inverter to Integrate Solar-Wind Hybrid fed DC-Grid with Distributed AC grid

Abhishek Awasthi
Dept. of Electrical Engineering, MNNIT,
Allahabad, India.
abhishekawasthi761993@gmail.com

Karthikeyan Venkitusamy
Dept. of Electrical Engineering, MNNIT,
Allahabad, India.
karthi13546@gmail.com

Rajasekar Selvamuthukumaran
Technology Dept., Power Grid Corporation of
India Limited, Gurgaon, India.
rajasekar6387@gmail.com

Sanjeevikumar Padmanaban
Research and Development
Ohm Technologies, Chennai, India.
sanjeevi_12@yahoo.co.in

Pierluigi Siano
Dept. of Industrial Engineering
University of Salerno, Salerno, Italy.
psiano@unisa.it

Ahmet H. Ertas
Dept. of Biomedical Engineering, Faculty of
Engineering, Karabuk University, Turkey
ahertas@karabuk.edu.tr

Abstract: This paper presents integration of solar-wind hybrid fed DC-grid to distributed AC grid. Generally, the renewable hybrid energy systems use two or more energy sources to supply power to the dc grid. In case of insufficient power generation or excessive load demand, in order to supply power to DC loads, it must integrate with AC grid. As dc loads increase in number, complexity increases and tighter voltage regulation is required. This paper presents dual mode control operation of inverter which integrates the solar and wind power fed dc bus to the single phase ac distribution system. The inverter can be operated in hysteresis current control when power is fed from DC grid to AC distributed grid and in AC-DC boost rectifier mode otherwise. The detailed operation of dual mode control of inverter is described in this paper. The effectiveness of the proposed system has been verified through simulation studies using MATLAB/SIMULINK.

Index terms: Dual mode control, DC-grid, distributed AC grid and bidirectional inverter.

I. INTRODUCTION

Rampant consumption of fossil fuels such as coal, petroleum, natural gas, etc., in the power generation sector poses an imminent threat to the natural environment [1, 2]. Increasing cost and scarcity of such fuels at remote locations impairs grid expansion in such areas. A promising solution to deal with this problem includes development of Distributed Energy Resources (DERs) or Distributed Generation (DG) systems such as solar, wind, geothermal, small hydro, etc. Out of these, solar and wind energy systems have shown enormous potential [3-9].

The inherent drawback of using renewable energy systems is the unpredictable output power variability, which depends on the seasonal weather cycle of any geographical region. Direct integration of renewable DERs into the grid may cause voltage fluctuations and inability to supply power for a long duration of time. In order to achieve reliable and quality power supply, power electronic based converters are installed for interfacing DERs to the electrical grid. Accelerated development and research in the field of power electronics in the past decade has made DG based power grid a viable future prospect [10-13]. Progress in academic research coupled with

incentives, benefits provided by the government has generated a lot of interest in this field. Ministry of New and Renewable Energy (MNRE) has proposed various initiatives and plans to develop India's renewable energy sector. India's plan to achieve a total solar capacity equal to 22 GW by 2022 under Jawaharlal Nehru National Solar Mission (JNNSM) [14] is one such example.

Renewable energy systems can be classified based on the variety of energy sources as i.) Stand-alone (Islanding mode of operation) and ii.) Grid connected. Stand-alone energy systems function independent of any support from the main utility. There is no export or import of power to or from the grid. It usually requires an energy storage system such as batteries to provide backup power. These batteries are costly, polluting and bulky Hybrid energy systems combine two or more DERs together, thereby elevating system reliability and also reduce size of energy storage systems. The Initial setup cost is high which discourages investment, although the operating and maintenance cost is affordable [15]. As the number of sources increases, so does the technological complexity.

It is estimated that DC loads such as LED lighting and plug-in electric vehicles (PEV) make up 30% of the world's total consumption, which would gradually increase to 80% in the future [16]. Popularization of high voltage DC (HVDC) transmission [17-19] has refueled interest in DC power grids, which makes it necessary to develop control techniques and conditioning units to achieve stringent voltage regulation at the DC bus in any DG system with renewable sources as the power generators. This paper presents a single-phase bidirectional converter for integrating DC and AC bus to maintain their voltage levels. The converter performs bidirectional single-phase operation, i.e., rectification and boost operation when exporting power from the AC grid to the DC bus and supplying current to the grid from the DC bus when power flows from the DC bus to AC bus.

II. SYSTEM DESCRIPTION

The Solar PV panel generates the power and delivers it to the DC bus via a single input Pulse Width Modulated (PWM)

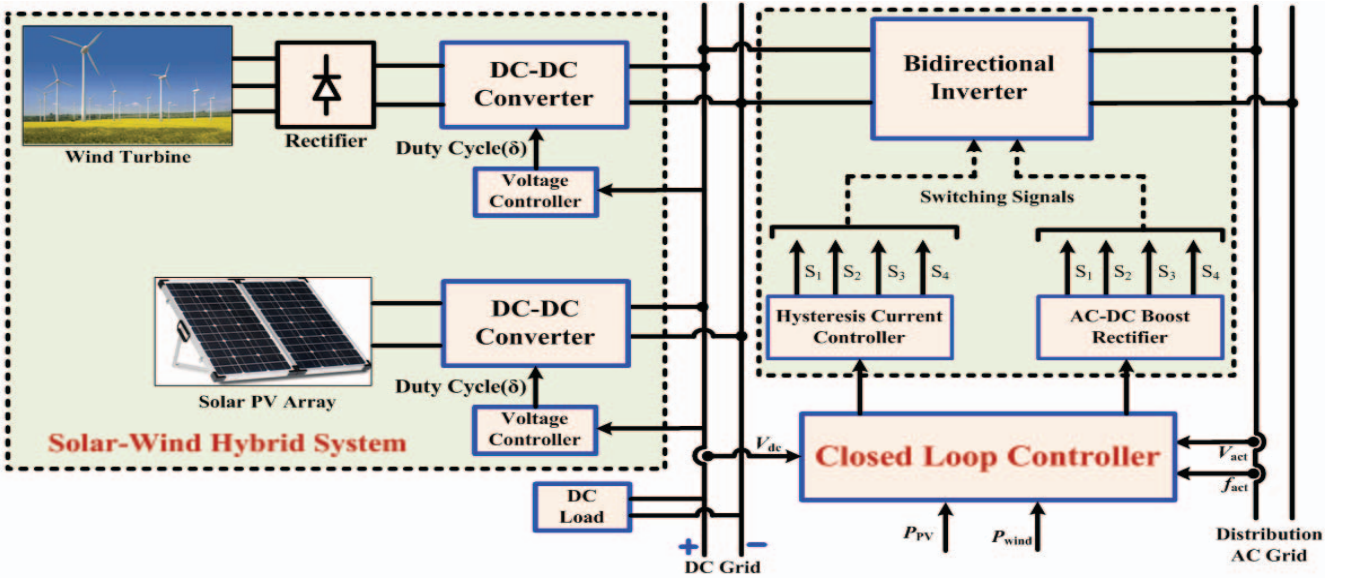


Fig. 1. Structure of distributed power generation.

DC/DC boost converter. The complete structure of the proposed system is shown in Fig. 1. It consists of Permanent Magnet Synchronous Generator (PMSG) based wind turbine energy conversion system supplies 3-phase AC voltage to a diode bridge rectifier (DBR). Its output DC voltage is stepped up equal to the voltage level of DC bus using DC/DC Boost converter. The voltage ripple is minimized in the process and normal operation is ensured. To mitigate the fluctuating input power supply and maintain a regulated voltage level at the DC bus, the boost converters operate in closed loop voltage control mode which provides the duty cycle of the PWM signal for the switch. The solar PV system generates DC supply. Energy from both these sources is fed through DC bus. A single phase inverter facilitates harmonized bi-directional power flow between the DC bus and AC distribution system, injecting sinusoidal AC current into the utility and maintaining the DC bus voltage in case any of the distributed sources fails. Closed loop controller guarantees bi-directional power flow, sensing DC voltage, AC voltage, frequency and power from solar PV and wind turbine for its continuous operation. The closed loop controller switches its functionality to a hysteresis current controller or AC/DC boost rectifier controller as per the required mode of operation.

A. Solar Energy

The solar energy is harnessed by solar PV modules composed of cells (generally made up of crystalline silicon) with efficiency in the range of 10-15%. Each solar cell is mathematically modeled as a current source in parallel connection with a diode. The current-voltage equation of a solar cell is given by the formula:

$$I_{pv} = I_{ph} - I_0 \left(e^{\frac{qV}{kT}} - 1 \right) \quad (1)$$

Where $I_{ph}(A)$ represents the photocurrent, $I_0(A)$ is the reverse saturation current of the diode, k is the Boltzmann

Constant= 1.38×10^{-23} (J/K), q is the electron charge= 1.6×10^{-19} (C) and T stands for the cell temperature (K) [20].

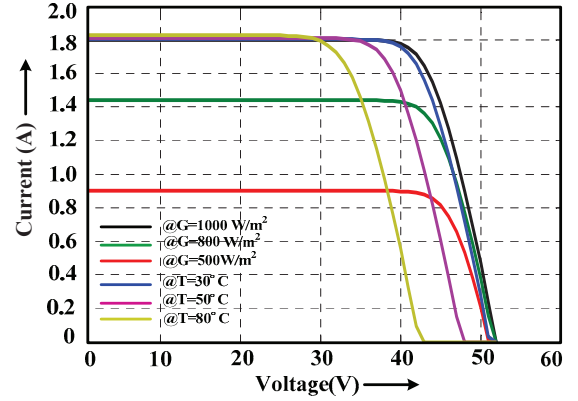


Fig. 2. I-V characteristics of solar PV.

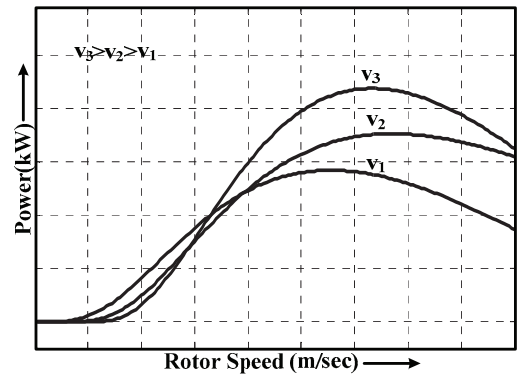


Fig. 3. C_p - λ curve of wind energy system.

A solar module is usually made up of 36 or 72 series connected PV cells. The cell circuits are protected by waterproof, sealed covering which ensures long life operation. Fig. 2 represents I-V characteristics of solar PV.

B. Wind Energy

The magnitude of the aerodynamic power, P is given by the following formula:

$$P = \frac{1}{2} \rho \pi C_p R^2 v^3 \quad (2)$$

where ρ is the atmospheric density, R represents turbine radius, v stands for wind speed, and C_p depends upon the tip speed ratio (λ) and blade pitch angle (β). Further, λ is defined as the ratio of tip speed of turbine blades to wind speed calculated as:

$$\lambda = \frac{R\Omega}{v} \quad (3)$$

where rotational speed of the wind turbine is represented as Ω . A characteristic plot between aerodynamic power, P and rotor speed, in Fig. 3 for different wind velocity v is shown [21].

III. CONCEPT OF INTEGRATION OF DC BUS WITH AC GRID

The DC distribution system supplying DC loads leads to 20% savings in the cost of components installed and an additional 8% reduction in power conversion losses [22]. The DC Bus voltage operates in the range of $360 \pm 20V$ by the DC link capacitors and is supplied by solar PV and wind turbines via power conditioning converters. The basic circuit configuration for the bidirectional inverter is shown in Fig. 4. A driver circuit provides the gating signals to the power electronic switches (MOSFET). The bidirectional inverter can be operated in two modes:

1. Hysteresis Current Control (HCC) Mode
2. AC/DC Boost Converter Mode

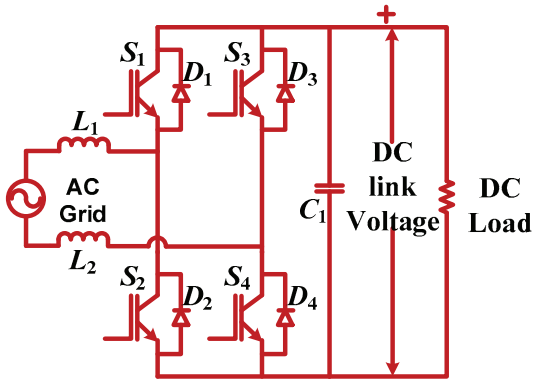


Fig. 4. Circuit configuration of bidirectional inverter.

A. Hysteresis Current Control Mode

In this mode, solar and wind power exceeds the power requirements by DC loads and the surplus power is fed into the AC distribution system through the bidirectional inverter. The closed loop controller operates as a fixed band hysteresis current controller, which tracks the reference current with a fixed tolerance band, shown in Fig. 5 and feeds the sinusoidal AC current into the grid.

Although HCC technique produces a large current ripple, yet ease of implementation and fast dynamic response overall leads to satisfactory results. The hysteresis current control is

more robust to uncertain parametric variations and provides over current protection without any supplementary component [23-25].

The relation between maximum switching frequency and hysteresis bandwidth is given by the relation [26]:

$$f_{\max} = \frac{V_{dc}}{4(L_T + L_s + (L_T L_s / L_l))h} \quad (4)$$

where L_s is feeder inductance, L_l is the line inductance, L_T is the interfacing inductance between the feeder and Voltage Source Inverter (VSI), V_{dc} is the dc link voltage across VSI, f_{\max} is the maximum switching frequency of the inverter and h is the hysteresis band width.

Since L_s equals zero for a stiff distribution system, the simplified expression is [27]:

$$f_{\max} = \frac{V_{dc}}{4L_T h} \quad (5)$$

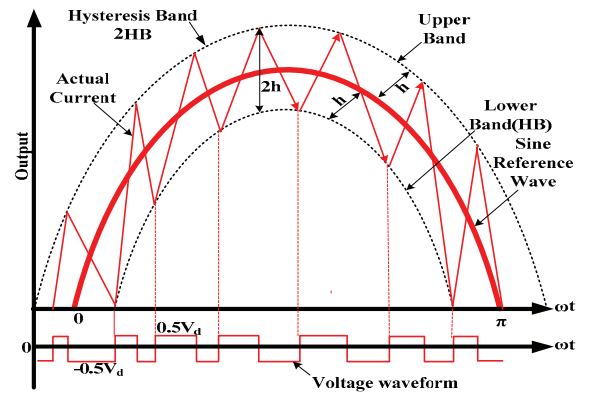


Fig. 5. Operating waveform of HCC.

B. AC/DC Boost Rectifier Mode

The inverter operates in this mode of operation when the distributed energy sources are unable to meet the demand by DC load due to failure of components or abrupt change in environmental conditions. The single phase bidirectional inverter can further undergo four different sub-modes of operation depends upon whether the inductor is in charge or discharging state. The switching frequency is fixed at 10 kHz. The capacitor undergoes charging/discharging $10 \text{ kHz}/50\text{Hz} = 200$ times per cycle.

Sub-Mode 1: In this mode of operation, positive half cycle of the AC grid voltage stores energy in inductor L_1 when switch S_2 is turned on and inductor L_1 charges. Grid current flows through inductor L_1 , switch S_2 , diode D_4 and inductor L_2 as shown in Fig. 6 (a). After the completion of the first cycle, DC link capacitor regulates DC bus voltage by discharging its stored energy. The upper legs of the single phase bidirectional inverter are not utilized during AC/DC boost rectification mode of operation.

Sub-Mode 2: In the discharging mode, diode D_4 is forward biased and DC link capacitor charges for a period of $(1-D) T_s$. Conduction path for the grid current is through inductor L_1 ,

diode D_1 , capacitor C_1 , diode D_4 and inductor L_2 , shown in Fig. 6(b).

Sub-Mode 3: Similar to mode 1, this mode of operation takes place when ac grid voltage across the inverter gets reversed during the negative half cycle. During this duration, inductor L_2 starts charging through switch S_4 for a period of DT_s sec., during this period the capacitor discharges continuously to maintain the DC bus voltage. Fig. 6(c) depicts current passing sequentially through inductor L_2 , switch S_4 , diode D_2 and inductor L_1 .

Sub-Mode 4: This mode of operation comes into play when the previously charged inductor L_2 starts dumping its stored energy across the dc link capacitor. The capacitor starts charging for a total period of $(1-D) T_s$ sec. The charging time constant is dependent on the conducting circuit resistance and the value of DC capacitance. Grid current flows through inductor L_2 , diode D_3 , capacitor C_1 , diode D_2 and inductor L_1 during this period as shown in Fig. 6(d). It is observed from Fig. 6 (a), Fig. 6(b), Fig. 6(c) and Fig. 6(d) that switches in

IV SIMULATION RESULTS

For the proposed system, simulation studies were performed using MATLAB/SIMULINK software. Under steady state operation, the simulation results of each stage are presented in this section. The simulation set up parameters of the system is tabulated in Table 1. Fig. 7 shows the 3-phase balanced AC voltages generated by the wind turbine fed PMSG with peak voltage of 300 V. The desired dc voltage of 360 V from DBR and solar PV fed boost converters is supplied to the DC distribution system with DC loads connected to it. Fig. 8 shows the DC bus voltage of 360 V with acceptable steady state ripple of 5%. The excess power is supplied to the AC distribution system via a bidirectional inverter. The AC Grid voltage during flow of power from DC

bus to AC bus reaches a maximum peak of 310 V which is approximately equal to $220 V_{RMS}$ as shown in Fig. 9 (a). When power flows from DC bus to AC bus or vice versa, it is necessary that the voltage levels of both the buses are properly regulated with minimum deviation from the reference voltages.

TABLE I. SIMULATION PARAMETERS.

Parameter	Value
Solar PV System	
Inductance (DC-DC boost converter)	500 μ H
Switching Frequency(boost converter)	10kHz
DC link Capacitance	1000 μ F
Wind System	
Inductance (DC-DC boost converter)	10mH
Switching Frequency(boost converter)	10kHz
DC link Capacitance	3000 μ F
Bidirectional Converter (Inverter)	
Switching Frequency	10kHz
Inductance (2Nos)	5mH
Capacitance	1000 μ F

The hysteresis current control is employed in order to feed desired current to the AC grid. Fig. 9 (b) depicts the injected AC current, which tracks the reference current equal to 6A. Fig. 9(c) portrays a magnified view which provides a better insight into the role of the hysteresis band in keeping the current ripple within the specified band width. In the situation when DC bus voltage falls due to unavailability or decrement of power from the renewable sources, power flows from AC to DC bus through the bidirectional inverter, which operates in the boost rectification mode. Fig. 10 (a) and (b) shows the pulsating DC voltage across the upper and lower leg switches of the inverter reaching a peak of 370 V. Fig. 9 (d) shows the voltage ripple is filtered by the DC link capacitor which settles to around 354 V, which is within the acceptable DC link voltage deviation limit.

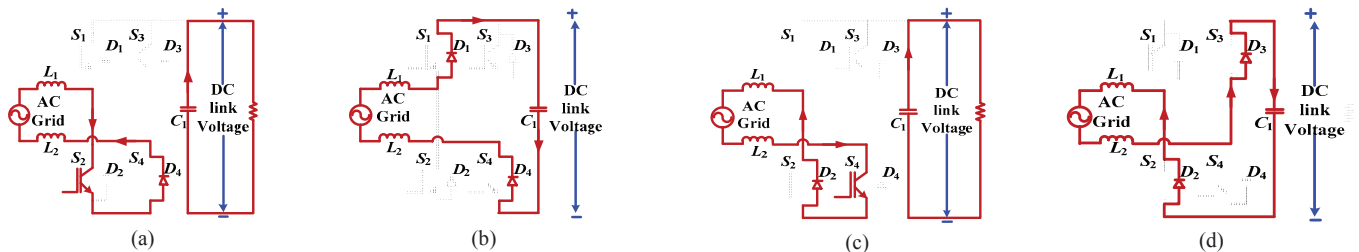


Fig. 6. Different modes of operation in AC-DC boost rectifier a) Sub- Mode 1, b) Sub-Mode 2, c) Sub-Mode 3, d) Sub-Mode 4.

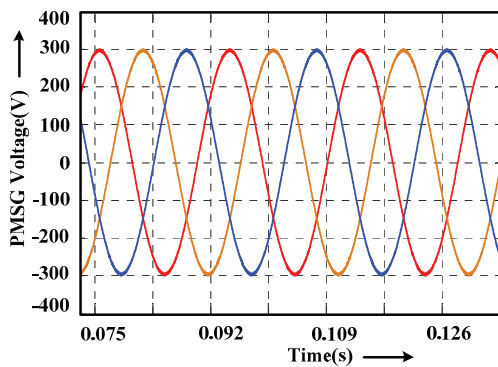


Fig. 7. PMSG output voltage waveform.

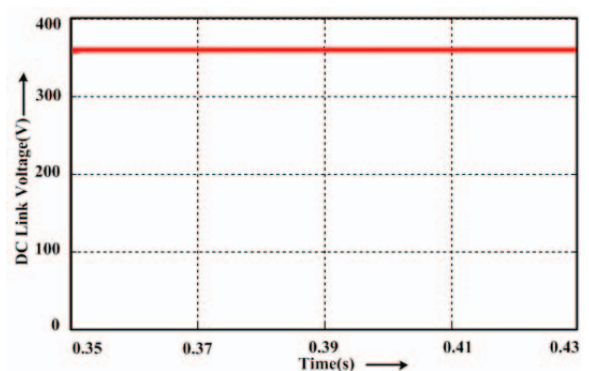


Fig. 8. DC link voltage during power flow from dc to ac side.

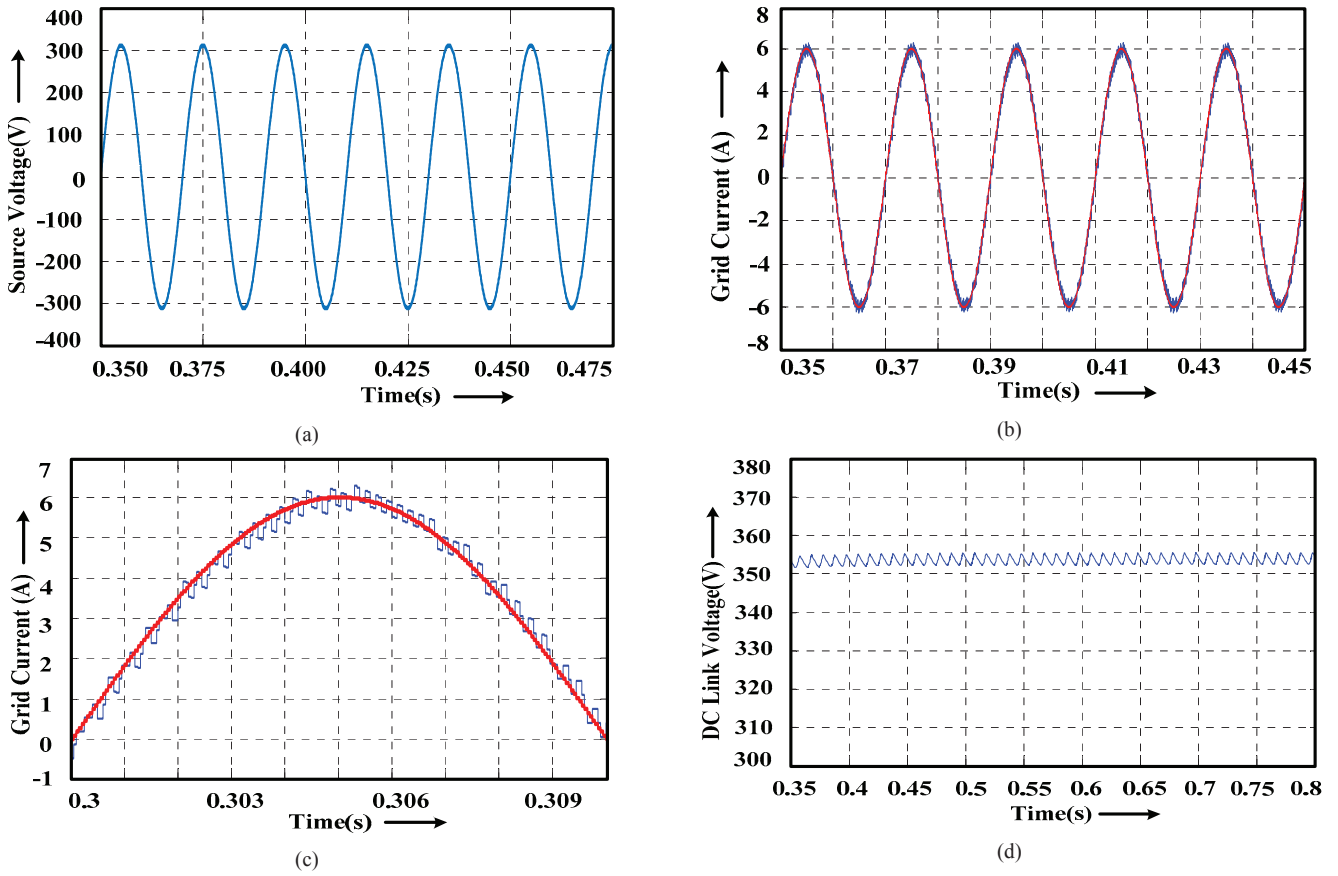


Fig. 9: Simulation results (a) AC Grid voltage during charging and discharging mode (b) AC Grid current while tracking (c) Magnified view of tracking (d) DC link voltage during inverter operation in ac/dc boost rectification mode.

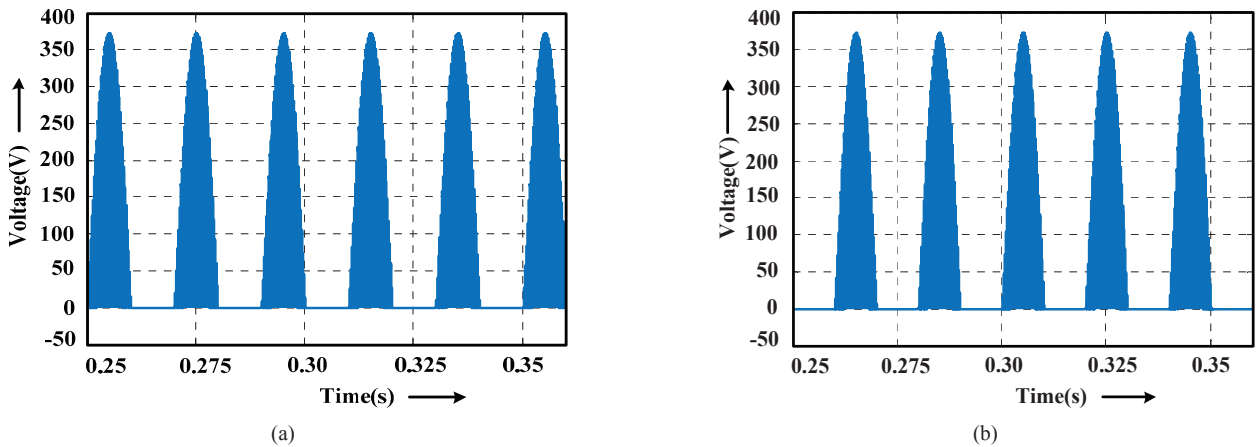


Fig. 10: Voltage waveform across (a) Switch S_1 (b) Switch S_2 .

V CONCLUSION

This paper proposes a dual mode control of bidirectional inverter to integrate Solar PV and wind fed DC bus with AC grid. The inverter operates in two modes, namely the hysteresis current control mode and as an AC/DC boost rectifier. The modes of operation have been studied in detail.

The latter mode of operation comes into play when there is hindrance in the power flow from the DG units, mainly because of weather conditions or failure of power conditioning units. Under such conditions, $220V_{RMS}$ at the grid needs to be rectified into DC while simultaneously maintaining the DC and AC bus voltage level. In order to verify the abovementioned operation, simulation results have been observed and presented.

REFERENCES

- [1] B. Bose, "Global warming: Energy, environmental pollution, and the impact of power electronics," *IEEE Ind. Electron. Mag.*, vol. 4, no. 1, pp. 6–17, Mar. 2010
- [2] Saifur Rahman and Arnulfo de Castro, "Environmental Impacts of Electricity Generation: A Global Perspective," *IEEE Trans. on Energy Conversion*, vol. 10, no. 2, pp. 307-314, Jun. 1995.
- [3] S. Kouro, J. I. Leon, D. Vinnikov, and L. G. Franque, "Grid-Connected Photovoltaic Systems: An Overview of Recent Research and Emerging PV Converter Technology," *IEEE Ind. Electronics Magazine*, vol. 9 no. 1, pp. 47–61, Mar. 2015.
- [4] L. Liu, H. Li, Y. Xue, and W. Liu, "Decoupled active and reactive power control for large-scale grid-connected photovoltaic systems using cascaded modular multilevel converters," *IEEE Trans. Power Electron.*, vol. 30, no. 1, pp. 176–187, Jan. 2015.
- [5] E. Romero Cadaval, G. Spagnuolo, L. G. Franquelo, C. A. Ramos-Paja, T. Suntio, and W. M. Xia, "Grid-connected photovoltaic generation plants: Components and operation," *IEEE Ind. Electron. Mag.*, vol. 7, no. 3, pp. 6–20, Sep. 2013.
- [6] P. P. Dash and M. Kazerani, "Dynamic modeling and performance analysis of a grid-connected current-source inverter-based photovoltaic system," *IEEE Trans. Sustain. Energy*, vol. 2, no. 4, pp. 443–450, Oct. 2011.
- [7] Z. Song, C. Xia, and T. Liu, "Predictive current control of three-phase grid-connected converters with constant switching frequency for wind energy systems," *IEEE Trans. Ind. Electron.*, vol. 60, no. 6, pp. 2451–2464, Jun. 2013.
- [8] L. Shang and J. Hu, "Sliding-mode-based direct power control of grid connected wind-turbine driven doubly fed induction generators under unbalanced grid voltage conditions," *IEEE Trans. Energy Convers.*, vol. 27, no. 2, pp. 362–373, Jun. 2012.
- [9] F. A. Ramirez, M. A. Arjona, "Development of a grid-connected wind generation system with a modified PLL structure," *IEEE Trans. Sust. Energy*, vol. 3, no. 3, pp. 474–81, May. 2012.
- [10] J.M. Carrasco, L.G. Franquelo, J.T. Bialasiewicz, E. Galvan, R. C. Portillo, M.A. M. Prats, J. I. Leon, and N. Moreno Alfonso, "Power electronic systems for the grid integration of renewable energy sources: A survey," *IEEE Trans. Ind. Electron.*, vol. 53, no. 4, pp. 1002-1016, Jun. 2006.
- [11] F. Blaabjerg, M. Liserre, and K. Ma, "Power electronics converters for wind turbine systems," *IEEE Trans. Ind. Appl.*, vol. 48, no. 2, pp. 708-719, Mar./Apr. 2012.
- [12] F. Blaabjerg, Z. Chen, and S.B. Kjaer, "Power electronics as efficient interface in dispersed power generation systems," *IEEE Trans. Power Electron.*, vol. 19, no. 5, pp. 1184-1194, Sept. 2004.
- [13] B. Bose, "Global energy scenario and impact of power electronics in 21st. century," *IEEE Trans. Ind. Electron.*, vol. 60, no. 7, pp. 2638–2651, Jul. 2013.
- [14] G. Shrimali, S. Rohra, "India's solar mission: A review," *Renewable and Sustainable Energy Reviews*, vol. 16, pp. 6317–6332, 2012.
- [15] T. Hirose and H. Matsuo, "Standalone hybrid wind-solar power generation system applying dump power control without dump load," *IEEE Trans. Ind. Electron.*, vol. 59, no. 2, pp. 988, 997, Feb. 2012.
- [16] G. F. Reed, "DC Technologies: Solutions to Electric Power System Advancements [Guest Editorial]," *Power and Energy Magazine, IEEE*, vol. 10, pp. 10 -17, Nov./Dec.2012
- [17] A. Glinkowski and C. Franck, "Guest editorial special section on HVDC systems and technologies," *IEEE Transactions on Power Delivery*, vol. 29, no. 1, pp. 307-309, 2014.
- [18] R. Majumder, C. Bartzsch, P. Kohnstam, E. Fullerton, A. Finn, and W. Galli, "Magic Bus: High -Voltage DC on the New Power Transmission Highway," *Power and Energy Magazine, IEEE*, vol. 10, pp. 39 -49, 2012.
- [19] E. Prieto-Araujo, F. Bianchi, A. Junyent-Ferre, and O. Gomis-Bellmunt, "Methodology for droop control dynamic analysis of multi terminal VSC-HVDC grids for offshore wind farms," *IEEE Trans. Power Del.*, vol. 26, no. 4, pp. 2476–2485, Oct. 2011.
- [20] Chetan Singh Solanki, "Solar Photovoltaic: Fundamentals, Technologies and application," PHI Learning Pvt., 2011.
- [21] J. F. Manwell, J. G. McGowan, and A. L. Rogers, "Wind Energy Explained: Theory, Design and Application," *John Wiley & Sons*, New York, NY, 2nd Edition, 2009.
- [22] T.-F. Wu, C.-H. Chang, L.-C. Lin, G.-R. Yu, and Y.-R. Chang, "DC-Bus Voltage Control With a Three-Phase Bidirectional Inverter for DC Distribution Systems," *IEEE Trans. Power Electronics*, vol. 28, no. 4, pp. 1890-1899, April 2013.
- [23] M. P. Kazmierkowski and L. Malesani, "Current control techniques for three-phase voltage-source PWM converters: A survey," *IEEE Trans. Ind. Electron.*, vol. 45, no. 5, pp. 691–703, Oct. 1998.
- [24] M. A. Rahman, T. S. Radwan, A. M. Osheiba, and A. E. Lashine, "Analysis of current controllers for voltage-source inverter," *IEEE Trans. Ind. Electron.*, vol. 44, no. 4, pp. 477–485, Aug. 1997.
- [25] S. Buso, S. Fasolo, L. Malesani, and P. Mattavelli, "A dead-beat adaptive hysteresis current control," *IEEE Trans. Ind. Appl.*, vol. 36, no. 4, pp. 1174–1180, Jul./Aug. 2000.
- [26] R. Gupta, "Generalized frequency domain formulation of the switching frequency for hysteresis current controlled VSI used for load compensation," *IEEE Trans. Power Electron.*, vol. 27, no. 5, pp. 2526–2535, May 2012.
- [27] M. K. Mishra and K. Karthikeyan, "An investigation on design and switching dynamics of a voltage source inverter to compensate unbalanced and nonlinear loads," *IEEE Trans. Ind. Electron.*, vol. 56, no. 8, pp. 2802–2810, Aug. 2009.